J. Mater. Environ. Sci. 5(4) (2014) 1133-1143
ISSN : 2028-2508
CODEN: JMESCN

Thermodynamic characterization of metal dissolution and inhibitor adsorption processes in mild steel / 3,5-bis(3,4-dimethoxyphenyl)-4-amino-1,2,4-triazole / hydrochloric acid system

M. Tourabi [a], K. Nohair [a], A. Nyassi [a], B. Hammouti [b], C. Jama [c], F. Bentiss [a,c,*]

[a] *Laboratoire de Catalyse et de Corrosion des Matériaux (LCCM), Faculté des Sciences, Université Chouaib Doukkali, B.P. 20, M-24000 El Jadida, Morocco*
[b] *LCAE-URAC18, Faculté des Sciences, Université Mohammed I[er] B.P. 717, M-60000 Oujda, Morocco*
[c] *UMET-ISP, CNRS UMR 8207, ENSCL, Université Lille Nord de France, BP 90108, F-59652 Villeneuve d'Ascq Cedex, France*

Received 22 Fev 2014, Revised 6 Mar 2014, Accepted 6 Mar 2014
** Corresponding author. E-mail address: fbentiss@enscl.fr*

Abstract
New 3,5-disubstituted-4-amino-1,2,4-triazole derivative, namely 3,5-bis(3,4-dimethoxyphenyl)-4-amino-1,2,4-triazole (3,4-MAT) was synthesised and its inhibitive action against the corrosion of mild steel in 1 M HCl solution was investigated at 308 K. The detailed study of 3,4-MAT was been performed using gravimetric measurements and polarisation curves method. Results show that 3,4-MAT is a good inhibitor and its inhibition efficiency reaches 98 % at $\cdot 10^{-3}$ M. Tafel polarisation study revealed that 3,4-MAT acts as a mixed type inhibitor. The inhibitor adsorption process in mild steel/3,4-MAT /hydrochloric acid system was studied at different temperatures (308-323 K) by means of weight loss measurements. The adsorption of 3,4-MAT on steel surface obeyed Langmuir's adsorption isotherm. The kinetic and thermodynamic parameters for mild steel corrosion and inhibitor adsorption, respectively, were determined and discussed

Key words: 4-aminotriazole; Mild steel; Hydrochloric acid; Corrosion inhibition; Adsorption.

1. Introduction
Acid solutions are widely used in industry for several purposes, such as acid pickling, industrial acid cleaning, acid descaling and oil well acidizing. Because of the general aggressively of acid solutions, inhibitors are commonly used to reduce the corrosive attack on metallic materials [1]. Inhibition appears to be the result of adsorption of molecules and ions on the metal surface [2]. Compounds with nitrogen and oxygen functional groups as well as multiple bonds or aromatic rings are considered to be one of the effective chemicals for inhibiting the metal corrosion [3–5]. Generally, the triazole derivatives on the corrosion inhibition of iron or steel in HCl and H_2SO_4 media have attracted more attention because of their excellent corrosion inhibition performance [6-23].
In continuation of our work on development of triazole derivatives as corrosion inhibitors in acidic media [6-17,24-26], we have studied the corrosion inhibiting behaviour of a new 3,5-disubstituted-4-amino-1,2,4-triazole derivative, namely 3,5-bis(3,4-dimethoxyphenyl)-4-amino-1,2,4-triazole (3,4-MAT), on mild steel in 1 M HCl medium. In the present work, the inhibition effect of 3,4-MAT on the corrosion of mild steel in 1 M HCl was studied using weight loss and potentiodynamic polarisation curves methods. Also, the effect of temperature on the corrosion rate was discussed. Both kinetic and standard thermodynamic parameters are calculated and discussed in detail.

2. Experimental details
2.1. Materials
The tested inhibitor, namely 3,5-bis(3,4-dimethoxyphenyl)-4-amino-1,2,4-triazole (3,4-MAT), was synthesised according to a previously described experimental procedure [27,28]. The molecular structure of 3,4-MAT is shown in Fig. 1. The structure of the 3,4-MAT was confirmed by ^{1}H and ^{13}C NMR, mass spectroscopy and elemental analysis.
The material used in this study is a mild steel with a chemical composition (in wt%) of 0.09% P, 0.38% Si, 0.01% Al, 0.05% Mn, 0.21% C, 0.05% S and the remainder iron (Fe). The steel samples were pre-treated prior to the experiments by grinding with emery paper SiC (120, 600 and 1200); rinsed with distilled water, degreased in acetone in an ultrasonic bath immersion for 5 min, washed again with bidistilled water and then dried at room temperature before use. The acid solutions (1 M HCl) were prepared by dilution of an analytical reagent grade 37 % HCl with doubly distilled water. The solubility of the 3,4-MAT is

about 10^{-4} M in 1 M HCl. The concentration range of 3,4-MAT employed was 10^{-6} M to 10^{-4} M in order to compare their corrosion inhibition properties with those of similar heterocyclic compounds.

2.2. Corrosion tests

The gravimetric measurements were carried out at the definite time interval of 4 h at room temperature using an analytical balance (precision ± 0.1 mg). Each run was carried out in a glass vessel containing 250 ml of the test solution. A clean weighed steel electrode (2 × 2 × 0.06 cm^3) was completely immersed at inclined position in the vessel. After the exposure time, the electrode was withdrawn, rinsed with doubly distilled water, washed with acetone, dried and weighed. Two batches of tests were performed, and the data reported in this paper represent the average value of the two tests. The weight loss (w), in mg, was taken as the difference in the weight of the mild steel coupons before and after immersion in different test solutions. Weight loss allowed calculation of the mean corrosion rate (C_R) in mg cm^{-2} h^{-1}.

Polarisation curves were conducted using an electrochemical measurement system EG§G potentiostat-galvanostat model 273A controlled by a PC supported by the 352 Soft Corr™ III Software. Electrochemical measurements were carried out in a conventional three-electrode cylindrical Pyrex glass cell. The temperature is thermostatically controlled at 308 K. The working electrode (WE) in the form of disc cut from steel has a geometric area of 1 cm^2 and is embedded in polytetrafluoroethylene (PTFE). A saturated calomel electrode (SCE) and a platinum electrode were used, as reference and auxiliary electrodes, respectively. A fine Luggin capillary was placed close to the working electrode to minimize ohmic resistance. All test solutions were de-aerated in the cell by using pure nitrogen for 30 min prior to the experiment. During each experiment, the test solution was mixed with a magnetic stirrer and the gas bubbling was maintained. The mild steel electrode was maintained at corrosion potential for 30 min and thereafter pre-polarised at –800 mV for 10 min. The potential was swept to anodic potentials by a constant sweep rate of 0.5 mV s^{-1}.

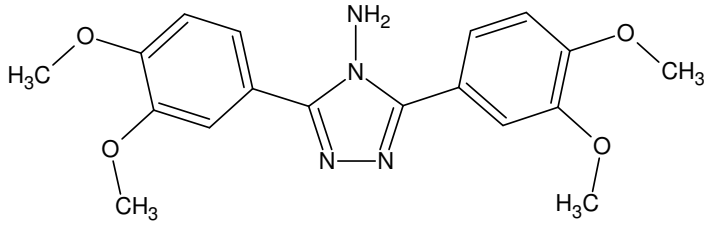

Figure 1: Chemical structure of 3,5-bis(3,4-dimethoxyphenyl)-4-amino-1,2,4-triazole (3,4-MAT).

3. Results and discussion

3.1. Effect of 3,4-MAT concentration

3.1.1. Weight loss study

The effect of addition of 3,5-bis(3,4-dimethoxyphenyl)-4-amino-1,2,4-triazole (3,4-MAT) tested at different concentrations on the corrosion of mild steel in 1 M HCl solution was studied by weight loss measurements at 308 K after 4 h of immersion period. The corrosion rate (C_R) and inhibition efficiency $\eta(\%)$ were calculated according to the Eqs. 1 and 2 [25], respectively:

$$C_R = \frac{W_b - W_a}{At} \quad (1)$$

$$\eta_{WL}(\%) = \left(1 - \frac{wi}{w_0}\right) \times 100 \quad (2)$$

where W_b and W_a are the specimen weight before and after immersion in the tested solution, w_0 and w_i are the values of corrosion weight losses of mild steel in uninhibited and inhibited solutions, respectively, A the area of the mild steel specimen (cm^2) and t is the exposure time (h).

Table 1: Corrosion parameters obtained from weight loss measurements for carbon steel in 1 M HCl containing various concentrations of 3,4-MAT at 308 K

Inhibitor	Concentration (M)	C_R (mg cm^{-2} h^{-1})	η_{WL} (%)
Blank	—	0.94	—
3,4-MAT	1×10^{-6}	0.379	59.7
	$5 \times .10^{-6}$	0.164	82.6
	1×10^{-5}	0.106	88.7
	5×10^{-5}	0.033	96.5
	1×10^{-4}	0.014	98.5

The values of percentage inhibition efficiency $\eta_{WL}(\%)$ and corrosion rate (C_R) obtained from weight loss method at different concentrations of 3,4-MAT at 308 K are summarized in Table 1. The variation of $\eta_{WL}(\%)$ with the 3,4-MAT concentration is shown in Fig. 2. It is very clear from theses results that the 3,4-MAT inhibits the corrosion of mild steel in1 M HCl solution, at all concentrations used in this study, and the corrosion rate (C_R) decreases continuously with increasing additive concentration at 308 K. Indeed, corrosion rate values of mild steel decrease when the inhibitor concentration increases while $\eta_{WL}(\%)$ values of 3,4-MAT increase with the increase of the concentration, the maximum $\eta_{WL}(\%)$ of 98.5 % is achieved at 10^{-4} M (Table 1, Fig. 2). The plausible mechanism for corrosion inhibition of mild steel in 1 M HCl by 3,4-MAT may be explained on the basis of adsorption of the 3,4-MAT molecule with the metal surface through the already adsorbed chloride ion. In acidic solutions, the 4-aminotiazole molecules exist as cations and adsorb through electrostatic interactions between the positively charged 3,4-MAT cations and adsorbed chloride ions [13]. Owing to the acidity of the medium, 3,4-MAT molecules can exist as a neutral species or in the cationic form. Thus, the adsorption of the neutral 3,4-MAT molecules could occur due to the formation of links between the d-orbital of iron atoms, involving the displacement of water molecules from the metal surface, and the lone sp^2 electron pairs present on the N and O atoms and π-orbitals, blocking the active sites in the steel surface and therefore decreasing the corrosion rate. Moreover, the presence of electron releasing character of $-OCH_3$ in the dimethoxyphenyl group may be attributed to the increased electron density leading to electron transfer mechanism from functional group to metal surface.

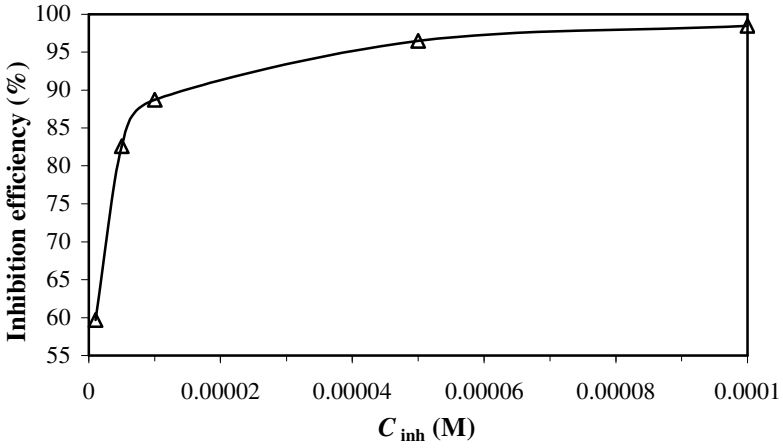

Figure 2: Variation of inhibition efficiency of mild steel in 1 M HCl containing various concentrations of 3,4-MAT.

In order to obtain a better understanding of the corrosion protection mechanism of 3,4-MAT against the corrosion of mild steel in normal hydrochloric medium, a detailed study on this inhibitor was carried out using Tafel polarisation and thermodynamic studies.

3.1.2. Tafel polarisation study

Polarization measurements have been carried out in order to gain knowledge concerning the kinetics of the anodic and cathodic reactions. Typical potentiodynamic polarization curves of the mild steel in 1 M HCl solutions without and with addition of different concentrations of 3,4-MAT are shown in Fig. 3. Electrochemical kinetic parameters (corrosion potential (E_{corr}), corrosion current density (I_{corr}) and cathodic Tafel slope (β_c)), determined from these experiments by extrapolation method [29], are reported in Table 2. The I_{corr} was determined by Tafel extrapolation of only the cathodic polarization curve alone, which usually produces a longer and better defined Tafel region [30]. The I_{corr} values were used to calculate the inhibition efficiency, $\eta_{Tafel}(\%)$, (listed in Table 2), using the following equation [31]:

$$\eta_{Tafel}(\%) = \frac{I_{corr} - I_{corr(i)}}{I_{corr}} \times 100 \quad (3)$$

where I_{corr} and $I_{corr(i)}$ are the corrosion current densities for steel electrode in the uninhibited and inhibited solutions, respectively.

Inspection of the figure 3 shows that the addition of 3,4-MAT has an inhibitive effect in the both anodic and cathodic parts of the polarization curves and generally shifted the E_{corr} value towards the positive direction compared to the uninhibited steel. Thus, addition of this inhibitor reduces the mild steel dissolution as well as retards the hydrogen evolution reaction. In addition, the parallel cathodic Tafel curves in Fig. 3 show that the hydrogen evolution is activation-controlled and the reduction mechanism is not affected by the presence of the inhibitor [17]. So, it could be

concluded that this 4-amino-1,2,4-triazole derivative (3,4-MAT) is of the mixed-type inhibitor for steel in 1 M HCl solution. Indeed, this inhibitor can exist as a cationic species in 1 M HCl medium, which may be adsorbed on the cathodic sites of the mild steel and reduce the evolution of hydrogen. Moreover, the adsorption of this compound on anodic sites through the lone pairs of electrons of nitrogen and oxygen atoms will then reduce the anodic dissolution of mild steel.

The analyse of the data in Table 2 revealed that the corrosion current density (I_{corr}) decreases considerably with increasing 3,4-MAT concentration, with a positive shift in corrosion potential (maximum displacement ≈ 100 mV) compared to that of uninhibited solution. The values of β_c show a slight change with increasing inhibitor concentration, indicating the influence of the aminotriazole derivative on the kinetics of hydrogen evolution. This may probably be due to a diffusion or barrier effect [32]. The dependence of $\eta_{Tafel}(\%)$ versus the inhibitor concentration of 3,4-MAT is also presented in Table 2. The obtained efficiencies indicate that 3,4-MAT acts as effective inhibitor. Indeed, the values of $\eta_{Tafel}(\%)$ increase with inhibitor concentration, reaching its maximum value, 91.8 %, at 10^{-4} M. The results (Tables 1 and 2) are in acceptable agreement with those obtained from weight loss study and show the same trend. The differences observed between the two types of experiments (Tables 1 and 2) are probably due to a greater extent to the different exposure time in the corrosive solution (1 h for the potentiodynamic and 4 h for the gravimetric measurements). Hence this factor does not affect the inhibition mechanism but influences only the kinetics of the processes.

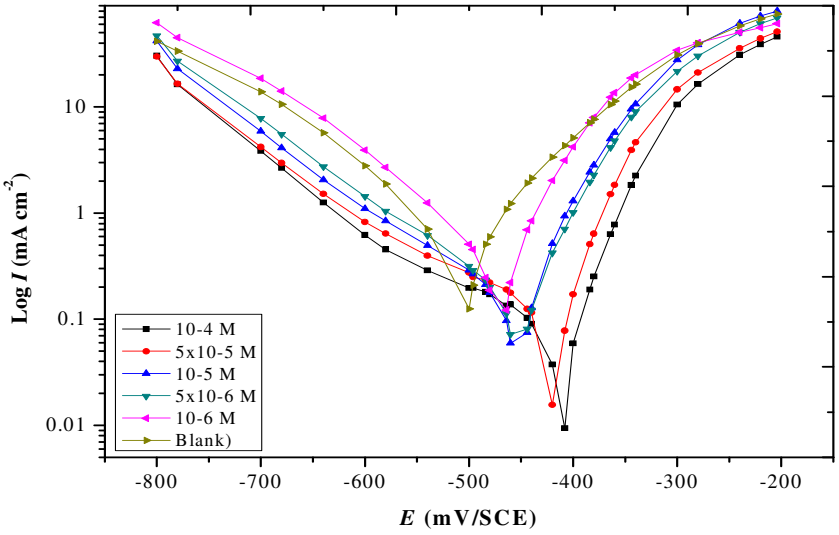

Figure 3: Typical polarisation curves for mild steel in 1 M HCl for various concentrations of 3,4-MAT at 308 K

Table 2: Polarisation parameters and the corresponding inhibition efficiency of mild steel corrosion in 1 M HCl containing different concentrations of 3,4-MAT at 308 K

Inhibitor	Concentration (M)	E_{corr} vs. SCE (mV)	$-\beta_c$ (mV dec^{-1})	i_{corr} (μA cm^{-2})	η_{Tafel} (%)
Blank	—	–513	139	624	—
3,4-MAT	1×10^{-6}	–470	120	322	48.4
	$5\times.10^{-6}$	–452	159	166	73.4
	1×10^{-5}	–453	176	157	74.8
	5×10^{-5}	–416	189	86	86.2
	1×10^{-4}	–411	174	51	91.8

3.2. Effect of temperature

3.2.1. Corrosion kinetic study

The effect of temperature on the inhibited acid–metal reaction is very complex, because many changes occur on the metal surface such as rapid etching, desorption of inhibitor and the inhibitor itself may undergo decomposition [33]. The change of the corrosion rate at selected concentrations of the 3,4-MAT during 4 h of immersion with the temperature was studied in 1 M HCl, both in absence and presence of inhibitor. For this purpose, gravimetric experiments were performed at different temperatures (308–323 K) and the results are given in Table 3.

Assuming that the corrosion rate of mild steel against the concentration of the studied inhibitor obeys the following kinetic relationship [34,35]:

$$\mathrm{Ln}C_{\mathrm{R}} = B\mathrm{Ln}C_{\mathrm{inh}} + \mathrm{Ln}k \quad (4)$$

where k is the rate constant and equal to C_{R} at inhibitor concentration of unity, B is the reaction constant which in the present case is a measure for the inhibitor effectiveness and C_{inh} is the inhibitor concentration.

Table 3: Corrosion parameters obtained from weight loss for mild steel in 1 M HCl containing various concentrations of 3,4-MAT at different temperatures

Concentration (M)	Temperature (K)	C_{R} (mg cm^{-2} h^{-1})	η_{WL} (%)	θ
Blank	308	0.940	—	—
	313	1.121	—	—
	318	1.166	—	—
	323	3.251	—	—
1×10^{-6}	308	0.379	59.7	0.597
	313	0.751	33.1	0.331
	318	0.982	15.7	0.157
	323	2.884	11.3	0.113
5×10^{-6}	308	0.164	82.6	0.826
	313	0.503	55.1	0.551
	318	0.851	27	0.27
	323	2.396	26.3	0.263
1×10^{-5}	308	0.106	88.7	0.887
	313	0.393	64.9	0.649
	318	0.671	42.5	0.425
	323	1.879	42.2	0.422
5×10^{-5}	308	0.033	96.5	0.965
	313	0.188	83.3	0.833
	318	0.275	76.4	0.764
	323	0.952	70.7	0.707
1×10^{-4}	308	0.014	98.5	0.985
	313	0.036	96.8	0.968
	318	0.148	87.3	0.873
	323	0.664	79.6	0.796

Figure 4 represents the curves of $\mathrm{Ln}C_{\mathrm{R}}$ versus $\mathrm{Ln}C_{\mathrm{inh}}$ at different studied temperatures. The straight lines show that the kinetic parameters (k and B) could be calculated by Eq. 4, and listed in Table 3.

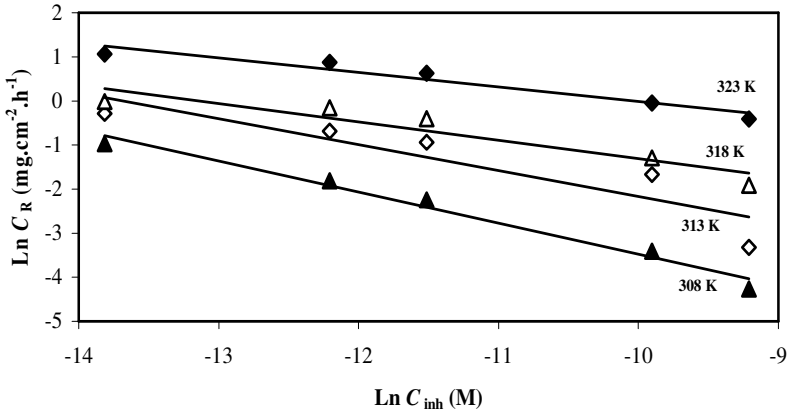

Figure 4: Variation of $\mathrm{Ln}C_{\mathrm{R}}$ with $\mathrm{Ln}C_{\mathrm{inh}}$ for mild steel in 1 M HCl containing 3,4-MAT at different temperatures.

The negative sign for the values of *B* indicates that the rate of corrosion process is inversely proportional to the inhibitor concentration, meaning that the inhibitor becomes more effective with increasing its concentration [34]. So, when the change of C_R with inhibitor concentration becomes steep (high negative value for constant *B*) it reflects good inhibitive properties for the studied inhibitor. Also, it is clear from Table 3 that the increase of corrosion rate (C_R) is more pronounced with the rise of temperature for blank solution. In the presence of the 3,4-MAT molecules, the corrosion rate of steel decreases at any given temperature as inhibitor concentration increases due to the increase of the degree of surface coverage. In contrast, at constant inhibitor concentration, the corrosion rate increases as temperature rises. Hence we note that the efficiency depends on the temperature and decreases with the rise of temperature from 308 to 323 K. This can be explained by the decrease of the strength of the adsorption process at elevated temperature and would suggest a physical adsorption mode.

Table 4: Kinetic parameters for the corrosion of mild steel in 1 M HCl containing 3,4-MAT at different temperatures

Temperature (K)	*B*	*k* (mg.cm^{-2}.h^{-1})
308	-0.704	-10.513
313	-0.588	-8.044
318	-0.417	-5.479
323	-0.330	-3.314

To calculate activation thermodynamic parameters of the corrosion process, Arrhenius Eq. (5 and transition state Eq. (6) were used [36]:

$$C_R = A \exp\left(-\frac{E_a}{RT}\right) \quad (5)$$

$$C_R = \frac{RT}{Nh}\exp\left(\frac{\Delta S_a}{R}\right)\exp\left(-\frac{\Delta H_a}{RT}\right) \quad (6)$$

where E_a is the apparent activation corrosion energy, *R* is the universal gas constant, *A* is the Arrhenius pre-exponential factor, *h* is Plank's constant, *N* is Avogrado's number, ΔS_a is the entropy of activation and ΔH_a is the enthalpy of activation.

Arrhenius plots for the corrosion rate of mild steel ($\ln(C_R)$ vs. $1/T$) are given in Fig. 5. Values of apparent activation energy of corrosion (E_a) for mild steel in 1 M HCl with the absence and presence of various concentrations of 3,4-MAT are calculated by linear regression between $\ln(C_R)$ and $1/T$ and the results are given in Table 5.

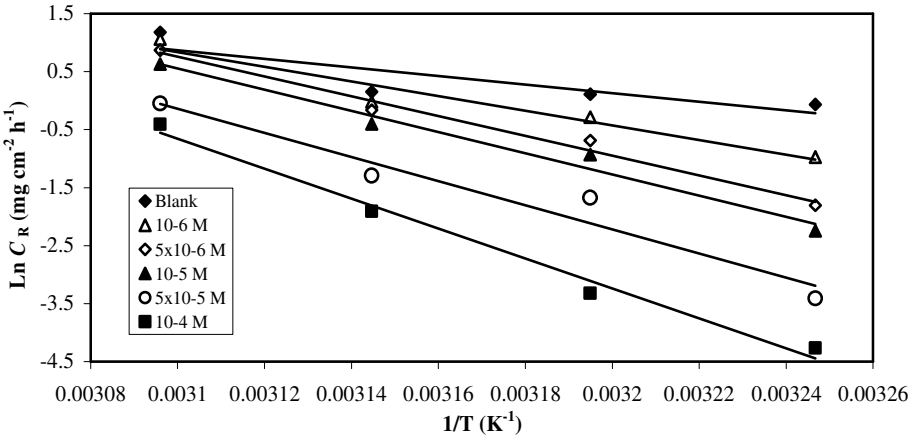

Figure 5: Arrhenius plots for mild steel corrosion rates (*C*R) in 1 M HCl in absence and in presence of different concentrations of 3,4-MAT.

All the linear regression coefficients are close to 1, indicating that the steel corrosion in hydrochloric acid can be elucidated using the kinetic model. The value of 61.77 kJ mol^{-1} obtained for the activation energy E_a of the corrosion process in 1 M HCl lies in the range of the most frequently cited values, the majority of which are grouped around 60 kJ mol^{-1} [37]. As observed from the Table 5, the E_a increased with increasing concentration of 3,4-MAT, but all values of E_a in the range of the studied concentration, were higher than that of the uninhibited solution (blank). The increase in E_a in the presence of 3,4-MAT may be interpreted as physical adsorption. Indeed, a higher energy barrier for the corrosion process in the inhibited solution is associated with physical adsorption or weak chemical bonding between the inhibitor species and the steel surface [38,39]. Szauer et al. explained that the increase in activation energy can be

attributed to an appreciable decrease in the adsorption of the inhibitor on the mild steel surface with the increase in temperature. A corresponding increase in the corrosion rate occurs because of the greater area of metal that is consequently exposed to the acid environment [40].

Table 5: Corrosion kinetic parameters for steel in 1 M HCl in absence and presence of different concentrations of 3,4-MAT

Concentration (M)	E_a (kJ mol^{-1})	ΔH_a (kJ mol^{-1})	ΔS_a (J mol^{-1} K^{-1})	E_a-ΔH_a (kJ mol^{-1})
Blank	61.77	59.15	–54.95	2.62
1×10^{-6}	104.93	102.30	78.54	2.63
$5 \times .10^{-6}$	141.80	139.18	192.21	2.62
1×10^{-5}	151.66	149.04	221.02	2.62
5×10^{-5}	173.38	170.76	282.67	2.62
1×10^{-4}	214.58	211.96	406.05	2.62

Fig. 6 shows a plot of ln (C_R/T) against $1/T$. A straight lines are obtained with a slope of ($-\Delta H_a/R$) and an intercept of (ln $R/Nh + \Delta S_a/R$) from which the values of ΔH_a and ΔS_a are calculated, are listed in Table 5. Inspection of these data reveals that the ΔH_a values for dissolution reaction of mild steel in 1 M HCl in the presence of DMAE are higher (102.3–211.96 kJ mol^{-1}) than that of in the absence of inhibitors (59.15 kJ mol^{-1}). The positive signs of ΔH_a values reflect the endothermic nature of the mild steel dissolution process suggesting that the dissolution of mild steel is slow [41] in the presence of inhibitor. All values of E_a are larger than the analogous values of ΔH_a indicating that the corrosion process must involved a gaseous reaction, simply the hydrogen evolution reaction, associated with a decrease in the total reaction volume [42]. Moreover, for all systems, the average value of the difference E_a - ΔH_a is about 2.62 kJ mol^{-1} which approximately around the average value of RT (2.62 kJ mol^{-1}); where T are in the range of the experimental temperatures, indicating that the corrosion process is a unimolecular reaction as it is characterized by the following equation [43].

Concerning the entropy of activation (ΔS_a), it is clear from Table 5 that a large positive value of ΔS_a is obtained in the presence of 3,4-MAT, while a negative value is observed in uninhibited solution. The increase of ΔS_a is generally interpreted as an increase in disorder as the reactants are converted to the activated complexes [37]. This observation is in agreement with the findings of other workers [44-47]. This behaviour can also be explained as a result of the replacement process of water molecules during adsorption of molecule inhibitor on the steel surface and therefore the increasing in entropy of activation was attributed to the increasing in solvent entropy [48].

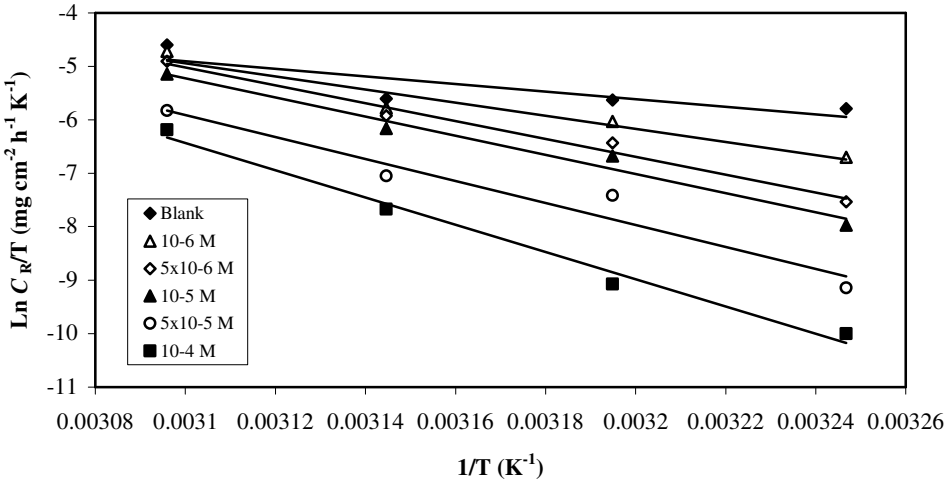

Figure 6: Transition-state plots for mild steel corrosion rates (C_R) in 1 M HCl in absence and in presence of different concentrations of 3,4-MAT.

3.2.2. Adsorption isotherm and thermodynamic parameters

The values of surface coverage θ corresponding to different concentrations of 3,4-MAT in the temperature range from 308 to 323 K have been used to explain the best isotherm to determine the adsorption process. The fractional surface coverage θ can be easily determined from weight loss measurements by the ratio η(%) / 100 (Table 3), if one assumes that the values of η(%) do no differ substantially from surface coverage (θ). As it is known that the adsorption of an organic adsorbate onto metal–solution interface can be presented as a substitutional adsorption process between the organic molecules in the aqueous solution $Org_{(sol)}$ and the water molecules on the metallic surface $H_2O_{(ads)}$:

$$Org_{(sol)} + n\,H_2O_{(ads)} \leftrightarrow Org_{(ads)} + n\,H_2O_{(sol)} \quad (7)$$

where $Org_{(sol)}$ and $Org_{(ads)}$ are the organic molecules in the aqueous solution and adsorbed on the metallic surface, respectively, $H_2O_{(ads)}$ is the water molecules on the metallic surface, n is the size ratio representing the number of water molecules replaced by one molecule of organic adsorbate. When the equilibrium of the process described in this equation is reached, it is possible to obtain different expressions of the adsorption isotherm plots, and thus the surface coverage degree (θ) can be plotted as a function of the concentration of the inhibitor under test [49]. The Langmuir adsorption isotherm was found to give the best description of the adsorption behaviour of 3,4-MAT. In This case, the surface coverage (θ) of the inhibitor on the steel surface is related to the concentration of inhibitor in the solution according to the following equation:

$$\frac{\theta}{1-\theta} = K_{ads} C_{inh} \quad (8)$$

Rearranging this equation gives:

$$\frac{C_{inh}}{\theta} = \frac{1}{K_{ads}} + C_{inh} \quad (9)$$

where θ is the surface coverage degree, C_{inh} is the inhibitor concentration in the electrolyte and K_{ads} is the equilibrium constant of the adsorption process. The K_{ads} values may be taken as a measure of the strength of the adsorption forces between the inhibitor molecules and the metal surface [50]. To calculate the adsorption parameters, the straight lines were drawn using the least squares method. The experimental (points) and calculated isotherms (lines) are plotted in Fig. 7. The results are presented in Table 6. A very good fit is observed with a regression coefficient (R^2) up to 0.98 and the obtained lines have slopes very close to unity, which suggests that the experimental data are well described by Langmuir isotherm and exhibit single-layer adsorption characteristic [33]. This kind of isotherm involves the assumption of no interaction between the adsorbed species and the electrode surface. From the intercepts of the straight lines C_{inh}/θ – axis, the K_{ads} values were calculated and given in Table 6. As can be seen from Table 3, K_{ads} values decrease with increasing temperature from 308 to 323 K. Such behaviour can be interpreted on the basis that the increase in the temperature results in desorption of some adsorbed inhibitor molecules from the metal surface [33].

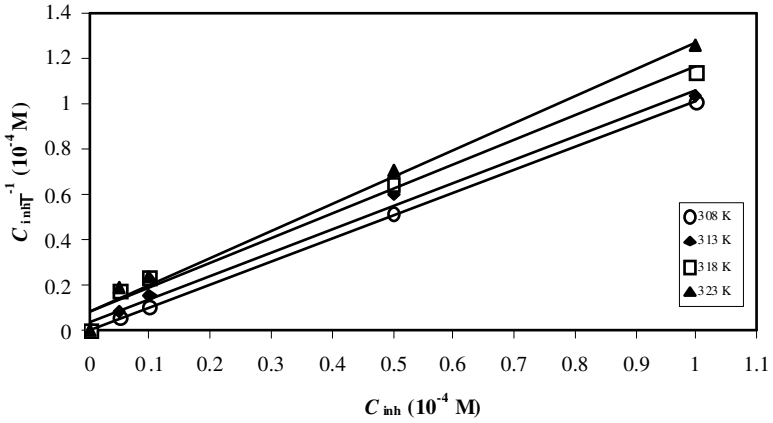

Figure 7: Langmuir's isotherm adsorption model of 3,4-MAT on the mild steel surface in 1 M HCl at different temperatures.

The well known thermodynamic adsorption parameters are the free energy of adsorption (ΔG^{o}_{ads}), the standard enthalpy of adsorption (ΔH^{o}_{ads}) and the entropy of adsorption (ΔS^{o}_{ads}). These quantities can be calculated depending on the estimated values of K_{ads} from adsorption isotherms, at different temperatures. The constant of adsorption, K_{ads}, is related to the standard free energy of adsorption, ΔG^{o}_{ads}, with the following equation [51]:

$$K_{ads} = \frac{1}{55.55} \exp\left(\frac{-\Delta G^{o}_{ads}}{RT}\right) \quad (10)$$

where R is the universal gas constant, T is the thermodynamic temperature and the value of 55.55 is the concentration of water in the solution in mol/l. The calculated ΔG^{o}_{ads} values, at all studied temperatures, are given in Table 6.

Generally, the adsorption type is regarded as physisorption if the absolute value of ΔG^0_{ads} is in the range of 20 kJ mol^{-1} or lower. The inhibition behaviour is attributed to the electrostatic interaction between the organic molecules and steel surface. When the absolute value of ΔG^0_{ads} is in the order of 40 kJ mol^{-1} or higher, the adsorption could be seen as chemisorption. In this process, the covalent bond is formed by the charge sharing or transferring from the inhibitor molecules to the metal surface [52,53]. The obtained ΔG^o_{ads} values in the studied temperature domain are in the range of –46.17 to –41.31 kJ mol^{-1}, indicating, therefore that the adsorption mechanism of the 3,4-MAT onto mild steel in 1 M HCl solution is mainly due to Chimisorption (Table 6). On the other hand, the obtained values of ΔG^o_{ads} generally show a regular dependence on temperature, indicating a good correlation among thermodynamic parameters.

Table 6: Thermodynamic parameters for the adsorption of 3,4-MAT on the mild steel in 1 M HCl at different temperatures

Temperature (K)	K_{ads} (10^4 M^{-1})	R^2	ΔG^o_{ads} (kJ mol^{-1})	ΔH^o_{ads} (kJ mol^{-1})	ΔS^o_{ads} (J mol^{-1}K^{-1})
308	121.95	0.999	–46.17	–132.55	-283.54
313	25.44	0.994	–42.84		
318	11.01	0.986	–41.31		
323	11.34	0.990	–42.04		

Thermodynamically, ΔG^o_{ads} is related to the standard enthalpy and entropy of the adsorption process, ΔH^o_{ads} and ΔS^o_{ads}, respectively, via Eq. (11):

$$\Delta G^o_{ads} = \Delta H^o_{ads} - T\Delta S^o_{ads} \quad (11)$$

and the standard enthalpy of adsorption (ΔH^o_{ads}) can be calculated according to the Van't Hoff equation [54]:

$$\ln K_{ads} = -\frac{\Delta H^o_{ads}}{RT} + \text{constant} \quad (12)$$

A plot of ln K_{ads} versus 1/T gives a straight line, as shown in Fig. 8. The slope of the straight line is $-\Delta H^o_{ads}/R$ and the intercept is ($\Delta S^o_{ads}/R$ + ln1/55.55). The obtained values of ΔH^o_{ads} and ΔS^o_{ads} are given in Table 6. Since the ΔH^o_{ads} value is negative, the adsorption of inhibitor molecules onto the mild steel surface is an exothermic process. In an exothermic process, chemisorption is distinguished from physisorption by considering the absolute value of ΔH^o_{ads}. For the chemisorption process, ΔH^o_{ads} approaches 100 kJ mol^{-1}; while for the physisorption process, it is less than 40 kJ mol^{-1} [55]. In the presented study, the calculated values of the ΔH^o_{ads} for the adsorption of 3,4-MAT is –132.55 kJ mol^{-1}, indicating that this inhibitor can be considered chemically adsorbed. The value of ΔS^o_{ads} is negative (Table 6), meaning that the inhibitor molecules move freely in the bulk solution (are chaotic) before adsorption, while as adsorption progresses, the inhibitor molecules adsorbed onto the mild steel surface become more orderly, resulting in a decrease in entropy [56]. This order may more probably be explained by the possibility of formation of iron-triazole complex on the metal surface [57].

ΔH^o_{ads} and ΔS^o_{ads} for the adsorption of 3,4-MAT on steel surface can be also deduced from Eq. (11). Fig. 9 shows the plot of ΔG^o_{ads} versus T which gives straight lines with slopes of $-\Delta S^o_{ads}$ and intercepts of ΔH^o_{ads}. The calculated ΔH^o_{ads} in this case is –130.93 kJ mol^{-1}, confirming the exothermic behaviour of the 3,4-MAT adsorption on the steel surface. Values of ΔH^o_{ads} obtained by the both methods are in good agreement. Moreover, the deduced ΔS^o_{ads} value of –278.4 J mol^{-1} K^{-1}, is very close to that obtained using the Van't Hoff equation (Table 6).

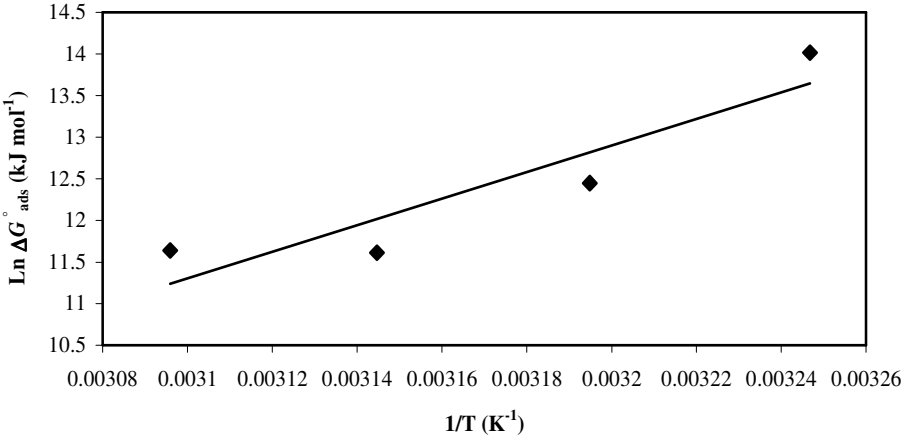

Figure 8: Vant't Hoff plot for the mild steel/3,4-MAT/1 M HCl system.

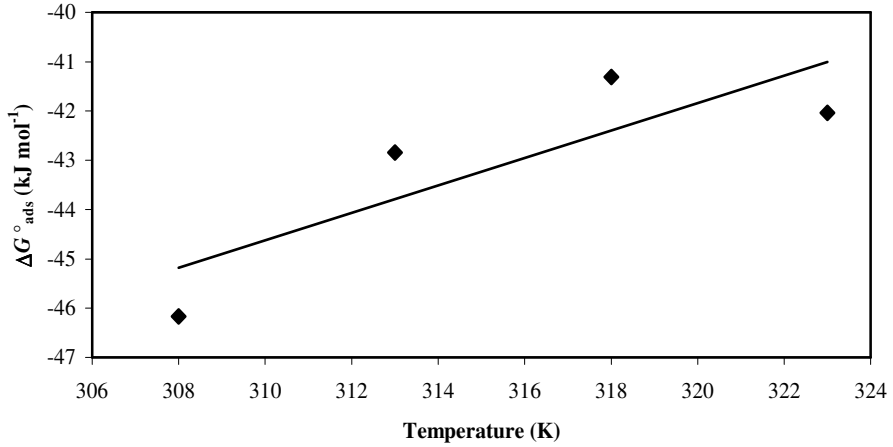

Figure 9: Variation of ΔG^{o}_{ads} versus *T* on mild steel in 1 M HCl containing 3,4-MAT.

Conclusion

3,5-bis(3,4-dimethoxyphenyl)-4-amino-1,2,4-triazole (3,4-MAT) shows excellent inhibition properties for the corrosion of mild steel in 1 M HCl at 308 K, and the inhibition efficiency, η(%), increases with increase of the 3,4-MAT concentration. At 10^{-4} M, the inhibition efficiency η(%) of 3,4-MAT, obtained by using gravimetric method, is as high as 98 %. The inhibitor efficiencies determined by weight loss and Tafel polarization methods are in reasonable agreement. Based on the Tafel polarization results, 3,4-MAT can be classified as mixed inhibitor. The inhibition efficiency of 3,4-MAT is found to decrease proportionally with increasing temperature (308 to 323 K) and its addition to 1 M HCl leads to increase of apparent activation energy (E_a) of corrosion process. The corrosion process is inhibited by the adsorption of 3,4-MAT on steel surface and the adsorption of the inhibitor fits a Langmuir kinetic/thermodynamic model under all of the studied temperatures. Thermodynamic adsorption parameters show that 3,4-MAT is adsorbed on mild steel surface by an exothermic process. Moreover, the calculated values of ΔG^{o}_{ads} and ΔH^{o}_{ads} reveal that the adsorption mechanism of 3,4-MAT on steel surface in 1 M HCl solution is mainly chemisorption.

References

1. Zhang, Q. B., Hua, Y. X., *Electrochim. Acta* 54 (2009) 1881.
2. Bentiss, F., Traisnel, M., Chaibi, N., Mernari, B., Vezin, H., Lagrenée, M., *Corros. Sci.* 44 (2002) 2271.
3. Ali, S. A., Saeed, M. T., Rahman, S. U., *Corros. Sci.* 45 (2003) 253.
4. Yildirim, A., Cetin, M., *Corros. sci.* 50 (2008) 155.
5. Bartos, M., Hackerman, N., *J. Electrochem. Soc.* 139 (1992) 3428.
6. Mernari, B., El Attari, H., Traisnel, M., Bentiss, F., Lagrenée, M., *Corros. Sci.* 40 (1998) 391.
7. Bentiss, F., Lagrenée, M., Traisnel, M., Mernari, B., El Attari, H., J. *Appl. Electrochem.* 29 (1999) 1073.
8. Bentiss, F., Lagrenée, M., Traisnel, M., Hornez, J. C., *Corros. Sci.* 41 (1999) 789.
9. Bentiss, F., Traisnel, M., Vezin, H., Lagrenée, M., *Indus. Eng. Chem. Res.* 39 (2000) 3732.
10. Bentiss, F., Traisnel, M., Lagrenée, M., *Brit. Corros. J.* 35 (2000) 315.

11. Bentiss, F., Traisnel, M., Gengembre, L., Lagrenée, M., *Appl. Surf. Sci.* 161 (2000) 194.
12. Bentiss, F., Bouanis, M., Mernari, B., Taisnel, M., Lagrenée, M., *J. Appl. Electrochem.* 32 (2002) 671.
13. Lagrenée, M., Mernari, B., Bouanis, M., Taisnel, M., Bentiss, F., *Corros. Sci.* 44 (2002) 573.
14. El Mehdi, B., Mernari, B., Traisnel, M., Bentiss, F., Lagrenée, M., *Mater. Chem. Phys.* 77 (2003) 489.
15. Bentiss, F., Bouanis, M., Mernari, B., Traisnel, M., Vezin, H., Lagrenée, M., *Appl. Surf. Sci.* 253 (2007) 3696.
16. Lebrini, M., Traisnel, M., Lagrenée, M., Mernari, B., Bentiss, F., *Corros. Sci.* 50 (2008) 473.
17. Bentiss F., Jama C., Mernari B., El Attari H., El Kadi L., Lebrini M., Traisnel M., Lagrenée M., *Corros. Sci.* 51 (2009) 1628.
18. Quraishi, M. A., Jamal, D., *Mater. Chem. Phys.* 68 (2001) 283.
19. Quraishi, M. A., Sharma, H. K., *Mater. Chem. Phys.* 78 (2003) 18.
20. Wang, H.-L., Fan, H.-B., Zheng, J.-S., *Mater. Chem. Phys.* 77 (2003) 655.
21. Zhang, S., Tao, Z., Liao, S., Wu, F., *Corros. Sci.* 52 (2010) 3126.
22. Musa A.Y., Kadhum A.A.H., Mohamad A.B., Takriff M.S., Daud A.R., Kamarudin S.K., *Corros. Sci.* 52 (2010) 526.
23. Musa, A. Y., Kadhum, A .A. H., Mohamad, A. B., Takriff, M. S., *Corros. Sci.* 52 (2010) 3331.
24 Tourabi. K., Nohair K., Nyassi N., Hammouti B., Bentiss F., Chetouani A., *Mor. J. Chem.* 1 (2013) 33.
25. Zarrok, H., Zarrouk, A., Hammouti, B., Salghi, R., Jama, C., Bentiss, F., *Corros. Sci.* 64 (2012) 243.
26. Tourabi, M., Nohair, K., Traisnel, M., Jama, C., Bentiss, F., *Corros. Sci.* 75 (2013) 123.
27. Bentiss, F., Lagrenée, M., Traisnel, M., Mernari, B., Elattari, H., *J. Heterocyclic Chem.* 36 (1999) 149.
28. Bentiss, F., Lagrenée, M., Barbry, D., *Tetrahedron Let.* 41 (2000) 1539.
29. Lebrini, M., Bentiss, F., Chihib, N., Jama, C., Hornez, J. P., Lagrenée, M., *Corros. Sci.* 50 (2008) 2914.
30. McCafferty E., *Corros. Sci.* 47 (2005) 3202.
31. Bouklah M., Benchat N., Aouniti A., Hammouti B., Benkaddour M., Lagrenée M., Vezin H., Bentiss F., *Prog. Org. Coat.* 51 (2004) 118.
32. Singh A. K., Quraishi, M. A., *Corros. Sci.* 52 (2010) 1529.
33. Bentiss F., Lebrini, M., Lagrenée, M., *Corros. Sci.* 47 (2005) 2915.
34. Noor E. A. *Corros. Sci.* 47 (2005) 33.
35. Boumhara K., Bentiss, F., Tabyaoui, M., Costa, J., Desjobert, J.-M., Bellaouchou, A., Guenbour, A., Hammouti, B., Al-Deyab S. S., *Inter. J. Electrochem. Sci.* 9(2014) 1187.
36. Bockris J. O'M., Reddy, A. K. N., Modern Electrochemistry, Plenum Press, New York, 2 (1977) 1267.
37. Herrag L., Hammouti, B., Elkadiri, S., Aouniti, A., Jama, C., Vezin, H., Bentiss, F., *Corros. Sci.* 52 (2010) 3042.
38. Popova A., Sokolova, E., Raicheva, S., Christov, M., *Corros. Sci.* 45 (2003) 33.
39. Elayyachy M., Elkodadi M., Aouniti A., Ramdani A., Hammouti B., Malek F., Elidrissi A., *Mat. Chem. Phys.* 93 (2005) 281.
40. Szauer T, Brand, A., *Electrochim. Acta* 26 (1981) 1219.
41. Guan N. M., Xueming, L., Fei, L., *Mater. Chem. Phys.* 86 (2004) 59.
42. Noor E.A., *Int. J. Electrochem. Sci.* 2 (2007) 996.
43. Gomma G. K., Wahdan, M. H., *Mater. Chem. Phys.* 39 (1995) 209.
44. Noor E. A., Al-Moubaraki, A. H., *Corros. Sci.* 51 (2009) 868.
45. Ahamad I., Prasad, R., Quraishi, M. A., *Corros. Sci.* 52 (2010) 933.
46. Popova A., Christov, M., Vasilev, A., *Corros. Sci.* 49 (2007) 3276.
47. Bouklah M., Benchat, N., Hammouti, B., Aouniti, A., Kertit, S., *Mater. Lett.* 60 (2006) 1901.
48. Ateya B., El-Anadouli, B. E., El-Nizamy, F. M., *Corros. Sci.* 24 (1984) 509.
49. Labjar N., Bentiss, F., Lebrini, M., Jama, C., El hajjaji, S., *Inter. J. Corros.* (2011), Article ID 548528.
50. Amin M. A., *J. Appl. Electrochem.* 36 (2006) 215.
51. El Azhar M., Traisnel, M., Mernari, B., Gengembre, L., Bentiss, F., Lagrenée, M., *App. Surf. Sci.* 185 (2010) 197.
52. Donahue F. M., Nobe, K., *J. Electrochem. Soc.* 112 (1965) 886.
53. Kamis E., Bellucci, F., Latanision, R. M., El-Ashry, E. S. H. *Corrosion* 47 (1991) 677.
54. Bouklah M., Hammouti, B., Lagrenée, M., Bentiss, F., *Corros. Sci.* 48 (2006) 2831.
55. Noor E. A., Al-Moubaraki, A. H., *Mater. Chem. Phys.* 110 (2008) 145.
56. Mu G., Li, X., Liu, G., *Corros. Sci.* 47 (2005) 1932.
57. Tang L., Li, X., Li, L., *Mater. Chem. Phys.* 97 (2006) 301.